Chapter 5

The Band Structure of the Electrons

5.1 Introduction

In the Fourier representation, i.e., in the basis of plane waves,

$$\chi_n(\mathbf{k}) = \frac{1}{\sqrt{V_g}} e^{i(\mathbf{k}+\mathbf{G}_n)\mathbf{r}} \tag{5.1}$$

the Hamilton operator of the Kohn-Sham equation has the form:

$$h_{n,m} = \frac{\hbar^2}{2m}(\mathbf{k}+\mathbf{G}_n)^2\delta_{n,m} + v^{\text{eff}}(\mathbf{G}_n - \mathbf{G}_m). \tag{5.2}$$

$v^{\text{eff}}(\mathbf{G}_n - \mathbf{G}_m)$ decreases with increasing length $|\mathbf{G}_n - \mathbf{G}_m|$, and thus $h_{n,m}$ is basically diagonal for large $|\mathbf{G}_n - \mathbf{G}_m|$. The corresponding eigenvalue equation enables the calculation of the energies and eigenfunctions for given $\mathbf{k}$.

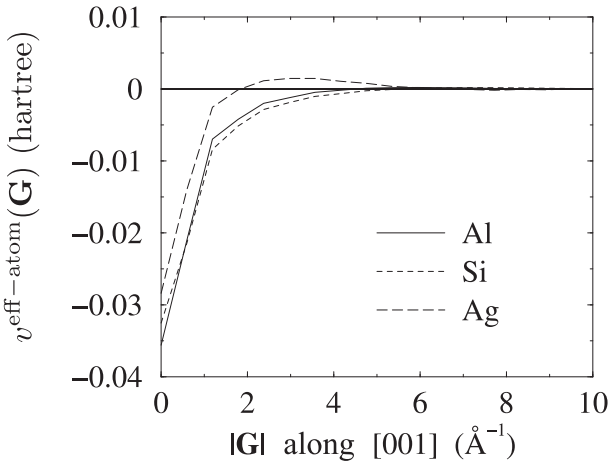

Figure 5.1: Fourier representation of the atomic potentials of Al, Si and Ag.

In Fig. 5.1 we show the function $v^{\text{eff}}(\mathbf{G})$ for three examples: Al, Si, and Ag. In fact, the figure shows the potential[1] of atoms and therefore, v^{eff} is defined for continuous values of $|\mathbf{G}|$. For a solid we have roughly

$$v^{\text{eff}}(\mathbf{r}) = \sum_{I=1}^{M} v^{\text{eff}-\text{atom}}(\mathbf{r} - \mathbf{R}_I) \quad ,$$

and then, in the Fourier representation $v^{\text{eff}-\text{atom}}$ is only needed at discrete reciprocal lattice vectors. These are determined by the lattice structure, and we have: $\frac{2\pi}{a} = 1.55$ Å^{-1}

[1]To be precise, Fig. 5.1 shows the effective potential for atomic pseudopotentials. The definition of pseudopotentials is given in Section *tba.* below.

(Al), 1.16 Å^{-1} (Si), and 1.54 Å^{-1} (Ag).

If *all* Fourier components $v^{\text{eff}}(\mathbf{G}_l)$ are small, we obtain the dispersion of free electrons:

$$\epsilon_n(\mathbf{k}) = \frac{\hbar^2}{2m}(\mathbf{k} + \mathbf{G}_n)^2. \tag{5.3}$$

$\epsilon_n(\mathbf{k})$ as a function of $\mathbf{k}$ is called the energy band n. For the one-dimensional case we have shown this dispersion before (cf. Fig. 4.13). However, the one-dimensional case is not typical, because in this case at most two-fold degeneracy can be present. Therefore, we will now discuss a two-dimensional example, which shows all the important characteristics of a band structure – even those of three-dimensional structures. We will investigate a hexagonal lattice. The 1st Brillouin zone and the labels of special k-points are shown in Fig. 5.2. If we now evaluate Eq. (5.3), we obtain the band structure of free electrons, as shown in Fig. 5.3, for $\mathbf{G}_0 = (0,0) = \Gamma$, $\mathbf{G}_1 = \frac{2\pi}{a}(0,1)$, $\mathbf{G}_2 = \frac{2\pi}{a}(\cos 30°, \sin 30°) = \frac{2\pi}{a}(\frac{\sqrt{3}}{2}, \frac{1}{2})$, $\mathbf{G}_3 = \frac{2\pi}{a}(\cos 30°, -\sin 30°) = \frac{2\pi}{a}(\frac{\sqrt{3}}{2}, -\frac{1}{2})$, etc. Here, we restrict ourselves to the boundary of the so-called *irreducible wedge*, which is hatched in Fig. 5.2. By reflection and rotation of this wedge the full 1st Brillouin zone can be obtained.

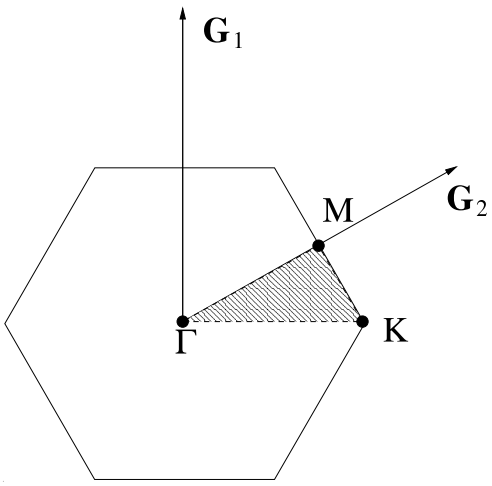

Figure 5.2: Brillouin zone of a hexagonal cell. Special **k**-points are shown. The hatched area is the irreducible part.

The point **K** is at $\frac{1}{3}(\mathbf{G}_2+\mathbf{G}_3) = \frac{2\pi}{a}(\frac{1}{\sqrt{3}}, 0)$, and along the $\overline{\Gamma\text{K}}$-direction we have $\mathbf{k} = (k_x, 0)$. We obtain the results:

$$\begin{aligned}
n=0, \quad \text{i.e.,} \quad \mathbf{G}_0: \quad \epsilon_0(\mathbf{k}) &= \tfrac{\hbar^2}{2m}k_x^2 \\
\epsilon_0(\Gamma) &= 0 \\
\epsilon_0(\text{K}) &= \tfrac{\hbar^2}{2m}(\tfrac{2\pi}{a}\tfrac{1}{\sqrt{3}})^2 \\
n=1, \quad \text{i.e.,} \quad \mathbf{G}_1: \quad \epsilon_1(\mathbf{k}) &= \tfrac{\hbar^2}{2m}(k_x^2 + (\tfrac{2\pi}{a})^2) \\
\epsilon_1(\Gamma) &= \tfrac{\hbar^2}{2m}(\tfrac{2\pi}{a})^2 \\
\epsilon_1(\text{K}) &= \tfrac{\hbar^2}{2m}(\tfrac{1}{3}+1)\cdot(\tfrac{2\pi}{a})^2
\end{aligned}$$

$$
\begin{aligned}
n=2, \quad \text{i.e.,} \quad \mathbf{G}_2: \quad \epsilon_2(\mathbf{k}) &= \frac{\hbar^2}{2m}\left\{\left(k_x+\frac{2\pi}{a}\frac{\sqrt{3}}{2}\right)^2+(\tfrac{2\pi}{a})^2\cdot\tfrac{1}{4}\right\} \\
\epsilon_2(\Gamma) &= \frac{\hbar^2}{2m}(\tfrac{2\pi}{a})^2(\tfrac{3}{4}+\tfrac{1}{4}) \\
&= \frac{\hbar^2}{2m}(\tfrac{2\pi}{a})^2=\epsilon_1(\Gamma) \\
\epsilon_2(\mathrm{K}) &= \frac{\hbar^2}{2m}(\tfrac{2\pi}{a})^2\cdot\tfrac{7}{3}
\end{aligned}
$$

etc.

The result for $\epsilon_n(\mathbf{k})$ is shown in Fig. 5.3. Even for free electrons the band structure – just because of the reduction to the 1st Brillouin zone – looks rather complicated.

Which modifications can we expect, if the potential – which has been zero so far – slightly differs from zero? This will be investigated in more detail now.

Plane waves with different $\mathbf{G}_n$ are coupled by the crystal potential (Bragg-condition, hybridization of states), i.e., wave functions and eigenvalues are different:

$$
\begin{aligned}
\tfrac{1}{\sqrt{V_\mathrm{g}}}e^{i(\mathbf{k}+\mathbf{G}_n)\mathbf{r}} \quad\longrightarrow\quad \varphi_{n,\mathbf{k}}(\mathbf{r}) &= \textstyle\sum_l c_{\mathbf{G}_n}(\mathbf{l})e^{i(\mathbf{k}+\mathbf{G}_l)\mathbf{r}}, \\
\epsilon_n(\mathbf{k}) &\longrightarrow \epsilon_n(\mathbf{k})+\Delta_n(\mathbf{k}) \quad .
\end{aligned}
$$

For non-degenerate states the change of the energy levels is small ($\sim v^{\mathrm{eff}}(\mathbf{G}_n)^2$), but it is larger for degenerate states[2] ($\sim v^{\mathrm{eff}}$):

$$
\Delta_n(\mathbf{k}) = \pm|v^{\mathrm{eff}}(\mathbf{G}_n)| \quad . \tag{5.4}
$$

Equation (5.4) describes the band structure close to the boundary of the 1st Brillouin zone. This is illustrated in Fig. 5.4. The representation of $\epsilon_n(\mathbf{k})$ in the domain of the 1st Brillouin zone is called a *reduced zone scheme*. Due to the equivalence of $\mathbf{k}$ and $(\mathbf{k}+\mathbf{G})$ we can consider the bands $\epsilon_n(\mathbf{k})$ also as periodic functions in $\mathbf{k}$-space, as shown in Fig. 5.5 for a one-dimensional example. However, the "repeated zone scheme" and the "extended

[2] cf. e.g. Ashcroft/Mermin, Chapter 9 or Madelung, Chapters 18–19.

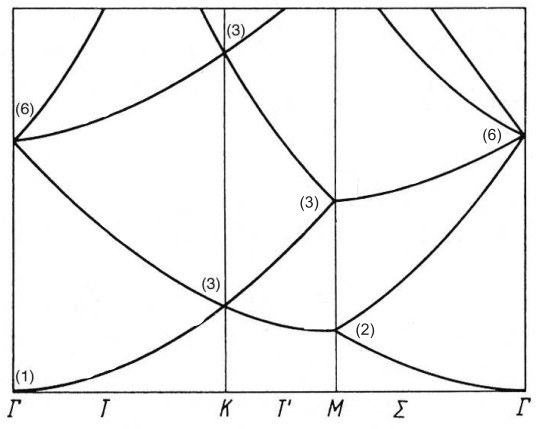

Figure 5.3: Band structure of free electrons in a hexagonal lattice. The numbers in brackets give the degeneracy.

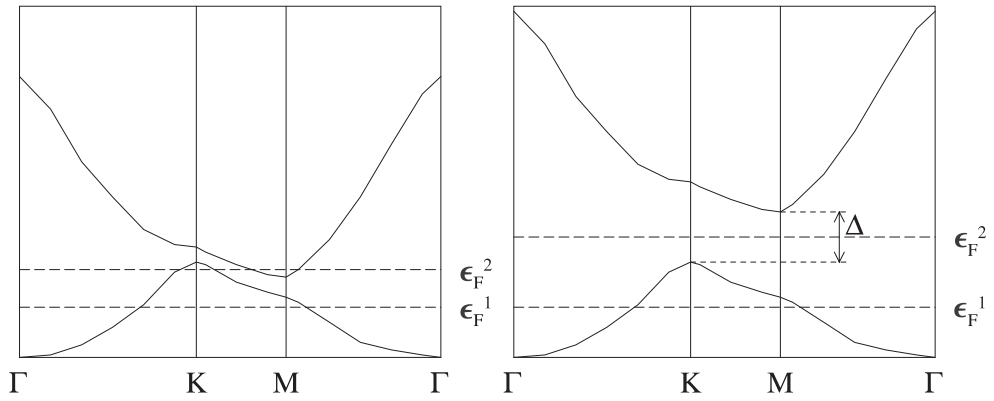

Figure 5.4: The band structure of *nearly* free electrons in a hexagonal lattice for two different systems and two different Fermi energies: ϵ_F^1 for 1 electron per cell and ϵ_F^2 for 2 electrons per cell.

zone scheme" illustrated in Fig. 5.5 are very rarely used.

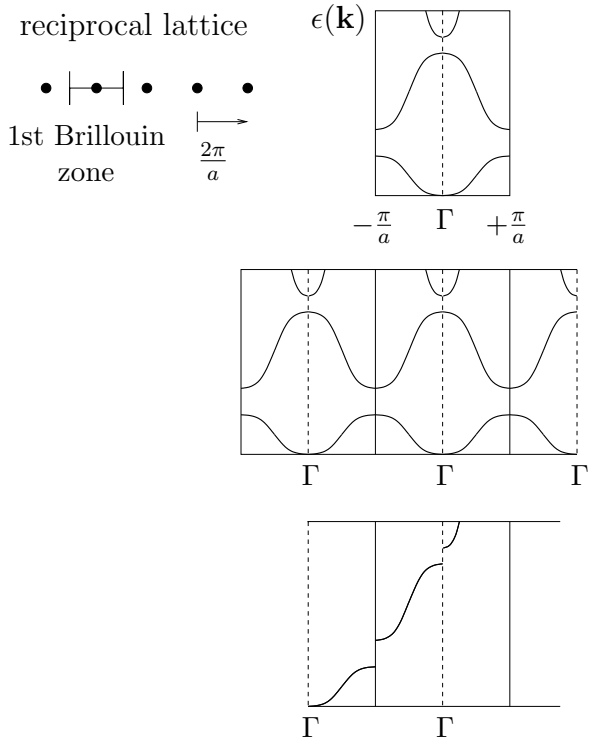

Figure 5.5: Three possible representations for $\epsilon_n(\mathbf{k})$ (one-dimensional example). **Top:** reduced zone scheme. **Middle:** repeated zone scheme. **Bottom**: extended zone scheme.

5.1.1 What Can We Learn from a Band Structure?

First we note that in a N electron system at $T = 0$ K the N lowest-energy states are occupied, i.e., each state $\varphi_{n,\mathbf{k}}(\mathbf{r})$ can be filled by two electrons: $\uparrow$ and $\downarrow$. One band, i.e., a

function $\epsilon_n(\mathbf{k})$ with fixed n but variable $\mathbf{k}$ ($\mathbf{k} \in$ 1st BZ), can be occupied by

$$2 \int\limits_{1.\mathrm{BZ}} \frac{V_\mathrm{g}}{(2\pi)^3} d^3k \tag{5.5}$$

electrons. The factor 2 takes into account the spin.

We have:

$$2 \int\limits_{1.\mathrm{BZ}} \frac{V_\mathrm{g}}{(2\pi)^3} d^3k = 2\frac{V_\mathrm{g}}{(2\pi)^3}\frac{(2\pi)^3}{\Omega} = 2\frac{V_\mathrm{g}}{\Omega} = 2\hat{N} \quad . \tag{5.6}$$

One band can be filled by $2\hat{N}$ electrons, where $\hat{N}$ is the number of unit cells in the base volume V_g, and Ω is the volume of the unit cell. Thus, one band can be filled by 2 electrons per primitive unit cell.

The number of electrons per primitive unit cell and the band structure determine important electric and optical properties of a solid, and we will now consider three special systems:

- **System #1: One electron per cell.**
  This can be, for example, alkali metals or noble metals (Cu, Ag, Au). The lowest band of the band structure is then half filled, i.e., the Fermi energy is in the middle of the band (cf. Fig. 5.4, ϵ_F^1). Thus, directly above the highest occupied state there are unoccupied states. The energy required to excite an electron (to give it a higher kinetic energy), therefore is arbitrarily small. Such a system is an electric conductor.

- **System #2: Two electrons per cell and a band structure as in Fig. 5.4, left.**
  If $\Delta < 0$, like in the left firgure of Fig. 5.4, the Fermi energy is at ϵ_F^2. Thus, the second band is partially filled while a fraction of the first band remains unoccupied. Also in this case the Fermi edge cuts bands, and thus also this system is a metal.

- **System #3: Two electrons per cell, and $\Delta > 0$ (Fig. 5.4, left).**
  Then, the lowest band is filled, and the Fermi energy is in the band gap above this band. The band occupied at $T = 0K$ is called *valence band* (VB), the unoccupied band above the band gap is called *conduction band* (CB). The position of the Fermi energy is then set equal to the chemical potential at $T = 0K$. In this case the electrons require an energy of at least $E_\mathrm{gap} = \Delta^\mathrm{KS} + \Delta_\mathrm{xc}$ for the excitation from an occupied to an unoccupied state. Here, Δ^KS is given by the Kohn-Sham eigenvalues calculated for the N-particle ground state:

$$\Delta^\mathrm{KS} \quad = \quad \epsilon^N_\mathrm{LB} - \epsilon^N_\mathrm{VB} \quad .$$

The quantity Δ_xc is introduced here because in principle Δ^KS does not correspond to an excitation. We will come back to this point in Section *tba.* below. Systems with $E_\mathrm{gap} \neq 0$ consequently are not electric conductors, but, depending on the size of the band gap $\Delta^\mathrm{KS} + \Delta_\mathrm{xc}$, they are called insulators or semiconductors.

The size of the band gap determines, for instance, the appearance of the material. The measured band gap is the difference between the ionization energy I (removal of an electron from the highest level of the valence band) and the affinity A (addition of an electron in the lowest level of the conduction band)[3]:

$$\begin{aligned} E_{\text{gap}} &= I - A \quad , & (5.7)\\ A &= E^N - E^{N+1} \quad , & (5.8)\\ I &= E^{N-1} - E^N \quad . & (5.9) \end{aligned}$$

From this we obtain

$$\begin{aligned} E_{\text{gap}} &= E^{N-1} - E^N + E^{N+1} - E^N \\ &= E^{N-1} + E^{N+1} - 2E^N \quad . & (5.10) \end{aligned}$$

Thus, for a correct evaluation of the band gap we need information for three different systems: The $N-1$, N, and the $N+1$ particle system. The Kohn-Sham eigenvalues are typically only evaluated for the N-particle system.

On the other hand for the Kohn-Sham eigenvalues we have:

$$\begin{aligned} A &= E^N - E^{N+1} \approx -\epsilon_{\text{CB}}^{N+\frac{1}{2}} \quad , & (5.11)\\ I &= E^{N-1} - E^N \approx -\epsilon_{\text{VB}}^{N+\frac{1}{2}} \quad , & (5.12) \end{aligned}$$

where we assumed that $E^{\tilde{N}}$ is continous and differentiable for $E^{N-1} < \tilde{N} < E^N$ and $E^N < \tilde{N} < E^{N+1}$. For integer values of $\tilde{N}$ this may not be the case (c.f. the discussion on the Janak-Slater transition state, Eq. (3.197)).

For the band gap we then obtain

$$\begin{aligned} E_{\text{gap}} &\approx \epsilon_{\text{CB}}^{N+\frac{1}{2}} - \epsilon_{VB}^{N-\frac{1}{2}} & (5.13)\\ &= \epsilon_{\text{CB}}^{N} - \epsilon_{\text{VB}}^{N} + \Delta_{\text{xc}} \quad . & (5.14) \end{aligned}$$

In the last line we used the Kohn-Sham eigenvalues only for the N-particle ground state and called the correction term Δ_{xc}.

At this point it is still controversially discussed if for the exact DFT the correction Δ_{xc} is there at all and, if it is, how big it may be. [4] For the known approximations of the xc functional it is quite clear, however, that the difference of the Kohn-Sham eigenvalues $(\epsilon_{\text{CB}}^N - \epsilon_{\text{VB}}^N)$ and the measured experimental band gap is indeed noticeable but much of this difference is due to the approximate treatment of xc. For the LDA, for example, the Kohn-Sham band gap underestimates the experimental band gap by about 50%. At this point, the only practical way to calculate a band gap is to leave DFT and to employ the many-body perturbation theory. Here, the so-called GW approximation (G is the Green function and W is the screened Coulomb interaction) is the state-of-the-art approach (see Section *tba.* below).

[3] I and A are both defined as positive quantities.

[4] For a recent discussion see P. Mori-Sanchez, A. J. Cohen, W. Yang, Phys. Rev. Lett. **100**, 146401 (2008).

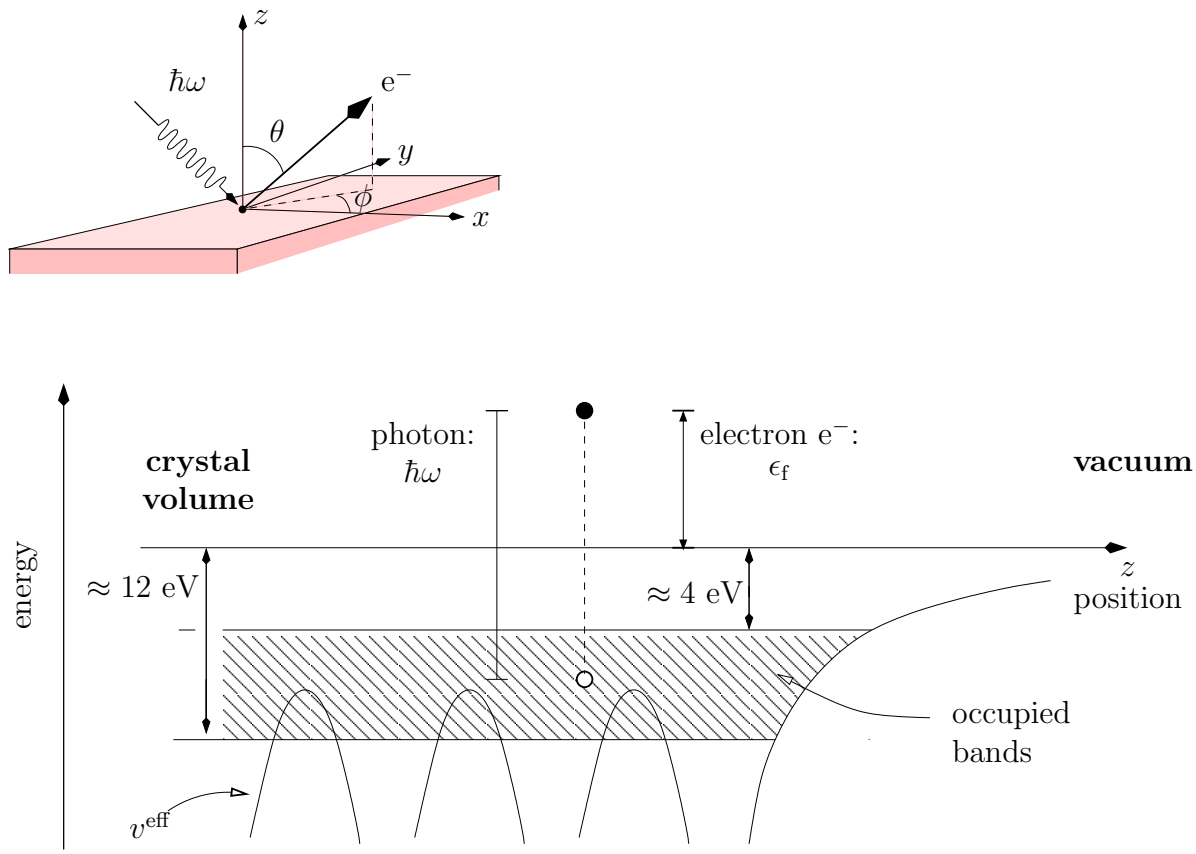

Figure 5.6: By measuring the intensity $I(\epsilon_\mathrm{f}, \theta, \phi, \hbar\omega, \mathbf{e})$ of the electrons emitted by an optical excitation $\hbar\omega$ (ϵ_f is the kinetic energy of the emitted electrons in vacuum; $\mathbf{e}$ and $\hbar\omega$ are the electric field vector and the energy of the light), information on the occupied states of the band structure can be obtained.

The quantity E_gap determines the appearance of the materials. If E_gap is lower than the energy of visible light[5], the solid looks like a metal (e.g. Si: $E_\mathrm{gap} = 1.1$ eV, or GaAs: $E_\mathrm{gap} = 1.45$ eV). If the band gap is in the range of visible light or larger, the solid is transparent to light (e.g. GaP: $E_\mathrm{gap} = 2.35$ eV looks orange because blue light is absorbed; diamond is clear and colorless: $E_\mathrm{gap} \approx 6$ eV). For semiconductors E_gap is in the order of $0.5 \ldots 5$ eV, so that at room temperature some electrons are excited (at 300 K we have $k_\mathrm{B} \cdot T = 0.026$ eV). For insulators we have: $E_\mathrm{gap} \gg k_\mathrm{B} \cdot T$. The term "semiconductor" is not well defined, i.e., strictly speaking a semiconductor is an insulator with a not too large band gap. In my view this is, however, not a useful definitiona. Much more relevant is the following: A semiconductor is an insulator that can be doped (i.e., impurity atoms can be added) to generate charge carriers in the valence band and/ or in the conduction band.

At the end of this paragraph we note that the band structure $\epsilon_n(\mathbf{k})$ can be studied experimentally. Angle-resolved photo emission (cf. Figs. 5.6 and 5.7) measures the electrons leaving the solid upon irradiation with light of energy $\hbar\omega$, mostly UV or X-rays. More precisely: One measures the kinetic energy ϵ_f of these electrons, the direction of their mo-

[5]Visible light is in the energy range $1.65 \text{ eV} < \hbar\omega < 3.1$ eV.

tion $\mathbf{k}_\mathrm{f}$ and their number per unit time (the index "f" ("final") refers to the final state). From this the energy of the occupied states $\epsilon_n(\mathbf{k}) \approx \epsilon_\mathrm{f} - \hbar\omega$ and of the corresponding $\mathbf{k}$-vectors can be determined. Such experiments require a tunable light frequency and thus a synchrotron. They are carried out for example at BESSY in Berlin, and at many other "synchrotron light sources" in the world.

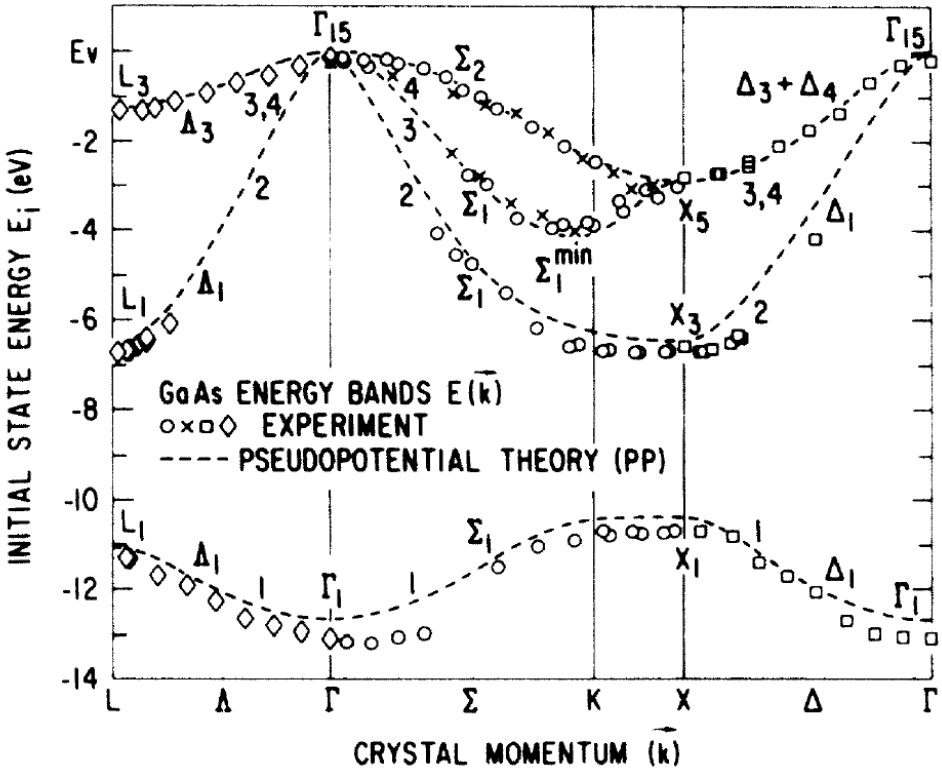

Figure 5.7: Comparison of a calculated empirical-pseudopotential band structure for GaAs (J.C. Phillips and K.C. Pandey, *Phys. Rev. Lett.* **30**, 787 (1973)) (dashed curve) with data measured by angle-resolved photo emission (T.C. Chiang, J.A. Knapp, M. Aono, and D.E. Eastman, *Phys. Rev. B* **21**, 3515 (1980)). For more recent band structures of the Kohn-Sham eigenvalues and using the LDA or the GGA the agreement is less good. In particular, the Kohn-Sham band gap between the top of the valence band and the bottom of the conduction band (not shown in the figure) is typically much smaller than the experimental one (at least when the LDA or GGA are used).

The theoretical band structure of Fig. 5.7 agrees very well with the experimental data. This clearly proves that the theory captures the right physics. However, the excellent quantitative agreement is also a consequence of the fact that this here was an *empirical* theory. *Ab initio* calculations are doing slightly worse for the bands. For the band gap, between VB and CB (not shown in Fig. 5.7), DFT is so far not doing well.

5.2 General Properties of $\epsilon_n(\mathbf{k})$

5.2.1 Continuity of $\epsilon_n(\mathbf{k})$ and Meaning of the First and Second Derivatives of $\epsilon_n(\mathbf{k})$

With

$$\varphi_{n,\mathbf{k}}(\mathbf{r}) = e^{i\mathbf{kr}} u_{n,\mathbf{k}}(\mathbf{r}) \tag{5.15}$$

we have

$$\begin{aligned} h\varphi_{n,\mathbf{k}}(\mathbf{r}) &= \left[-\tfrac{\hbar^2}{2m}\nabla^2 + v^{\text{eff}}(\mathbf{r})\right] e^{i\mathbf{kr}} u_{n,\mathbf{k}}(\mathbf{r}) \\ &= e^{i\mathbf{kr}} \left[-\tfrac{\hbar^2}{2m}\nabla^2 + v^{\text{eff}}(\mathbf{r}) + \tfrac{\hbar^2}{2m}k^2 - 2\tfrac{\hbar^2}{2m} i\mathbf{k}\boldsymbol{\nabla}\right] u_{n,\mathbf{k}}(\mathbf{r}) \qquad (5.16) \\ &= \epsilon_n(\mathbf{k}) e^{i\mathbf{kr}} u_{n,\mathbf{k}}(\mathbf{r}) \quad . \end{aligned}$$

Thus

$$\epsilon_n(\mathbf{k}) = \int_{V_g} u^*_{n,\mathbf{k}}(\mathbf{r}) \cdot \tilde{h}\, u_{n,\mathbf{k}}(\mathbf{r}) d^3\mathbf{r} \quad , \tag{5.17}$$

with

$$\tilde{h}(\mathbf{k}) \equiv \left[-\frac{\hbar^2}{2m}\nabla^2 + v^{\text{eff}}(\mathbf{r}) + \frac{\hbar^2}{2m}k^2 - 2\frac{\hbar^2}{2m} i\mathbf{k}\boldsymbol{\nabla}\right] \quad . \tag{5.18}$$

Thus, $\tilde{h}(\mathbf{k})$ determines the eigenvalue problem for given vectors $\mathbf{k} \in$ BZ:

$$\tilde{h}(\mathbf{k}) u_{n,\mathbf{k}} = \epsilon_n(\mathbf{k}) u_{n,\mathbf{k}} \quad , \tag{5.19}$$

for which we only have to consider one primitive unit cell because $u_{n,\mathbf{k}}(\mathbf{r})$ is periodic. In order to investigate the analytical properties of $\epsilon_n(\mathbf{k})$ we look at the neighborhood of an arbitrary point $\mathbf{k}$. For $\mathbf{k} + \boldsymbol{\kappa}$ we then have

$$\epsilon_n(\mathbf{k} + \boldsymbol{\kappa}) = \int u^*_{n,\mathbf{k}+\boldsymbol{\kappa}}(\mathbf{r}) \tilde{h}(\mathbf{k} + \boldsymbol{\kappa}) u_{n,\mathbf{k}+\boldsymbol{\kappa}}(\mathbf{r}) d^3r \quad . \tag{5.20}$$

As long as $|\boldsymbol{\kappa}|$ is small, the difference between $\tilde{h}(\mathbf{k})$ and $\tilde{h}(\mathbf{k} + \boldsymbol{\kappa})$

$$\tilde{h}(\mathbf{k} + \boldsymbol{\kappa}) - \tilde{h}(\mathbf{k}) = \frac{\hbar^2}{2m}(\kappa^2 + 2\mathbf{k}\boldsymbol{\kappa}) - \frac{\hbar^2}{2m} 2i\boldsymbol{\kappa}\boldsymbol{\nabla} \tag{5.21}$$

is also small. It seems reasonable to calculate the energy $\epsilon_n(\mathbf{k} + \boldsymbol{\kappa})$ by perturbation theory, i.e., to expand the functions $u_{n,\mathbf{k}+\boldsymbol{\kappa}}(\mathbf{r})$ with respect to the functions $u_{n,\mathbf{k}}(\mathbf{r})$ of the unperturbed problem:

$$\begin{aligned} \epsilon_n(\mathbf{k} + \boldsymbol{\kappa}) &= \underbrace{\int u^*_{n,\mathbf{k}}(\mathbf{r}) \tilde{h}(\mathbf{k}) u_{n,\mathbf{k}}(\mathbf{r}) d^3r}_{\text{0. Order}} \\ &\quad + \underbrace{\int u^*_{n,\mathbf{k}}(\mathbf{r}) \left\{\frac{\hbar^2}{2m}(\kappa^2 + 2\mathbf{k}\boldsymbol{\kappa}) - \frac{\hbar^2}{2m} 2i\boldsymbol{\kappa}\boldsymbol{\nabla}\right\} u_{n,\mathbf{k}}(\mathbf{r}) d^3r}_{\text{1. Order}} \end{aligned}$$

$$+ \underbrace{\sum_{m\neq n} \frac{\left|\int u^*_{n,\mathbf{k}}(\mathbf{r})\{\frac{\hbar^2}{2m}(\kappa^2+2\mathbf{k}\boldsymbol{\kappa})-\frac{\hbar^2}{2m}2i\boldsymbol{\kappa}\boldsymbol{\nabla}\}u_{m,\mathbf{k}}(\mathbf{r})d^3r\right|^2}{\epsilon_n(\mathbf{k})-\epsilon_m(\mathbf{k})}}_{\text{2. Order}}$$

$$+ \quad O(\kappa^3) \quad . \tag{5.22}$$

For convenience we now introduce the matrix element of the momentum operator:

$$\begin{aligned} \mathbf{p}_{nm} &= \langle\varphi_{n,\mathbf{k}}(\mathbf{r})|\frac{\hbar}{i}\boldsymbol{\nabla}|\varphi_{m,\mathbf{k}}(\mathbf{r})\rangle \\ &= \langle u_{n,\mathbf{k}}(\mathbf{r})|\hbar\mathbf{k}+\frac{\hbar}{i}\boldsymbol{\nabla}|u_{m,\mathbf{k}}(\mathbf{r})\rangle \quad , \end{aligned} \tag{5.23}$$

where the second equals sign is obtained from Bloch theorem. If we put Eq. (5.23) in Eq. (5.22) we obtain:

$$\begin{aligned} \epsilon_n(\mathbf{k}+\boldsymbol{\kappa})-\epsilon_n(\mathbf{k}) &= \frac{\hbar}{m}\boldsymbol{\kappa}\mathbf{p}_{nn}+\frac{\hbar^2}{2m}\kappa^2 \\ &+ \frac{\hbar^2}{2m}\sum_{m\neq n}\frac{|\boldsymbol{\kappa}\mathbf{p}_{nm}|^2}{\epsilon_n(\mathbf{k})-\epsilon_m(\mathbf{k})}+O(\kappa^3) \quad . \end{aligned} \tag{5.24}$$

The limit $|\boldsymbol{\kappa}| \longrightarrow 0$ illustrates that $\epsilon_n(\mathbf{k})$ is continuous as a function of $\mathbf{k}$, and that it is differentiable. Furthermore, we obtain the gradient $\boldsymbol{\nabla}_\mathbf{k}$ of $\epsilon_n(\mathbf{k})$:

$$\mathbf{p}_{nn} = \frac{m}{\hbar}\boldsymbol{\nabla}_\mathbf{k}\epsilon_n(\mathbf{k}) \quad . \tag{5.25}$$

The expectation value of the momentum operator therefore is not $\sim\mathbf{k}$, like for free electrons, but it is given by the gradient of the function $\epsilon_n(\mathbf{k})$. This is a rather important modification and, e.g., it may occur that $\mathbf{p}_{nn}$ decreases with increasing $\mathbf{k}$.

For the second derivative of the energy $\epsilon_n(\mathbf{k})$ with respect to $\mathbf{k}$ from Eq. (5.24) in the limit $|\boldsymbol{\kappa}| \longrightarrow 0$ we obtain:

$$\frac{\partial^2}{\partial k_\alpha \partial k_\beta}\epsilon_n(\mathbf{k}) = \frac{\hbar^2}{m}\delta_{\alpha\beta}+\frac{\hbar^2}{m}\sum_{m\neq n}\frac{\mathrm{Re}\,(p_{\alpha,nm}p^*_{\beta,nm})}{\epsilon_n(\mathbf{k})-\epsilon_m(\mathbf{k})} \quad . \tag{5.26}$$

For free electrons the second term on the right side of Eq. (5.26) vanishes, and the expression corresponds to the inverse of the inert mass of an electron. Close to maxima or minima of the band structure Bloch electrons behave as if they had a direction-dependent mass given by the tensor (5.26): This effective mass contains the effects due to the electron-lattice interaction and the electron-electron interaction. Using this concept (Eq. 5.26) and if we are interested in electronic states and their behavior at band extrema, the Hamilton operator can be simplified:

$$h = -\frac{\hbar^2}{2m}\nabla^2+v^{\mathrm{eff}}(\mathbf{r}) \quad \longrightarrow \quad \hat{h} = -\frac{\hbar^2}{2m^*}\nabla^2 \quad , \tag{5.27}$$

with

$$\frac{1}{m^*} = \frac{1}{\hbar^2}\frac{\partial^2\epsilon_n(\mathbf{k})}{\partial k_\alpha \partial k_\beta} \quad . \tag{5.28}$$

Here $\frac{1}{m^*}$ is a tensor and the expression is reasonable only in the part of the Brillouin zone, where $\epsilon_n(\mathbf{k})$ to a good approximation has a parabolic shape. This is obviously a severe limitation, but in some later parts of this lecture the concept of the effective mass will prove useful.

In Fig. 5.8 we show the lower edges of the conduction bands of two semiconductors. An electron at the bottom of the conduction band of silicon (left figure) has a larger effective mass than an electron at the bottom of the conduction band in GaAs (right figure). Thus, the conduction band electrons in GaAs mobility is larger.

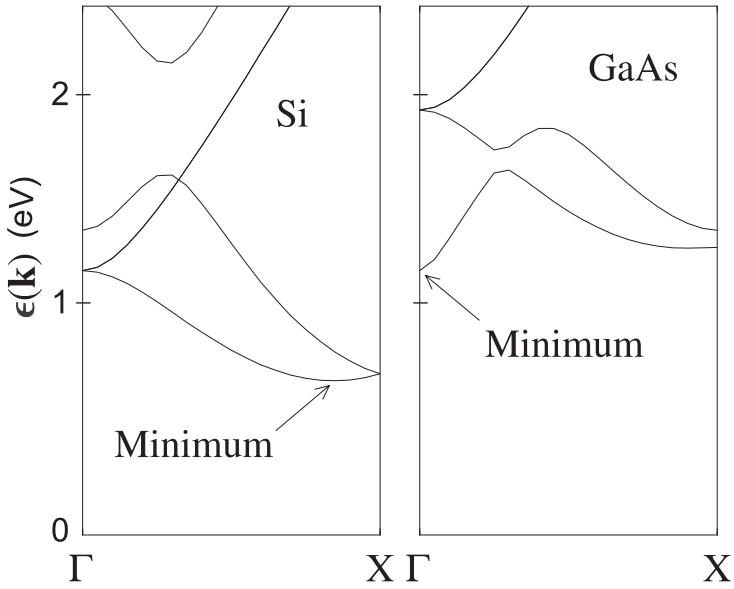

Figure 5.8: Band structure of the lower conduction band for two semiconductors, left Si and right GaAs. For the left system at the minimum the curvature is small. Thus, $1/m_{\text{eff}}$ is small, i.e., m_{eff} is large and the mobility of the charge carriers in this state is low. For the right system at the minimum the opposite is true, i.e., the mobility of the charge carriers at the minimum of the right system is high.

5.2.2 Time Reversal Symmetry

Further important properties of $\epsilon_n(\mathbf{k})$ are found when we consider the operation of time reversal T_t[6]:

$$T_t : \quad t \longrightarrow -t \quad . \tag{5.29}$$

This operator reverses the state of motion. For the time-independent Schrödinger equation this has the consequence that, since the position operator is invariant, spin and momentum operator change signs.

At first we want to investigate a system *without spin-orbit-coupling*, for which we have the Hamilton operator:

$$h = h^* \quad . \tag{5.30}$$

[6]cf. Madelung I., p. 107; Tinkham, p. 143.

We investigate two possibly different eigenfunctions of h, $\varphi_n(\mathbf{k},\mathbf{r})$ and $\varphi_n^*(\mathbf{k},\mathbf{r})$. Both functions are degenerate, because we have

$$h\varphi_n(\mathbf{k},\mathbf{r}) = \epsilon_n(\mathbf{k})\varphi_n(\mathbf{k},\mathbf{r}) \quad , \tag{5.31}$$

and with Eq. (5.30) conjugate complex:

$$h^*\varphi_n^*(\mathbf{r}) = h\varphi_n^*(\mathbf{k},\mathbf{r}) = \epsilon_n(\mathbf{k})\varphi_n^*(\mathbf{k},\mathbf{r}) \quad . \tag{5.32}$$

Are $\varphi_n(\mathbf{k},\mathbf{r})$ and $\varphi_n^*(\mathbf{k},\mathbf{r})$ physically different eigenfunctions? To answer this question we apply the translation operator to both functions:

$$T_{\mathbf{R}_I}\varphi_n(\mathbf{k},\mathbf{r}) = e^{\mathbf{ikR_I}}\varphi_n(\mathbf{k},\mathbf{r}) \quad , \tag{5.33}$$

or

$$T_{\mathbf{R}_I}\varphi_n^*(\mathbf{k},\mathbf{r}) = e^{-\mathbf{ikR_I}}\varphi_n^*(\mathbf{k},\mathbf{r}) \quad . \tag{5.34}$$

On the other hand we have:

$$T_{\mathbf{R}_I}\varphi_n(-\mathbf{k},\mathbf{r}) = e_I^{-\mathbf{ikR}}\varphi_n(-\mathbf{k},\mathbf{r}) \quad . \tag{5.35}$$

For $\varphi_n(\mathbf{k},\mathbf{r})$ we thus have the quantum numbers n and $\mathbf{k}$. On the other hand, for $\varphi_n^*(\mathbf{k},\mathbf{r})$ and for $\varphi_n(-\mathbf{k},\mathbf{r})$ the quantum numbers are n and $-\mathbf{k}$. Thus, $\varphi_n^*(\mathbf{k},\mathbf{r})$ is identical to $\varphi_n(-\mathbf{k},\mathbf{r})$. The energies of $\varphi_n(\mathbf{k},\mathbf{r})$ and of $\varphi_n(-\mathbf{k},\mathbf{r}) = \varphi_n^*(\mathbf{k},\mathbf{r})$ are $\epsilon_n(\mathbf{k})$ and $\epsilon_n(-\mathbf{k})$, and with Eq. (5.31) we obtain:

$$\epsilon_n(\mathbf{k}) = \epsilon_n(-\mathbf{k}) \quad . \tag{5.36}$$

This degeneracy is often given also because of spatial inversion symmetry, but what we have just found is also valid if the crystal does not have spatial inversion symmetry.

Now we investigate the Hamilton operator of a single-particle problem *with Spin-Orbit-Coupling*:

$$h = \left[-\frac{\hbar^2}{2m}\nabla^2 + v^{\text{eff}}(\mathbf{r})\right]\begin{pmatrix} 1 & 0 \\ 0 & 1 \end{pmatrix} + \frac{\hbar^2}{4m^2c^2}\boldsymbol{\sigma}(\boldsymbol{\nabla}v^{\text{eff}}(\mathbf{r}) \times \frac{\hbar}{i}\boldsymbol{\nabla}) \quad , \tag{5.37}$$

where the components of $\boldsymbol{\sigma}$ have the form

$$\sigma_x = \begin{pmatrix} 0 & 1 \\ 1 & 0 \end{pmatrix} \quad , \quad \sigma_y = \begin{pmatrix} 0 & -i \\ i & 0 \end{pmatrix} \quad , \quad \sigma_z = \begin{pmatrix} 1 & 0 \\ 0 & -1 \end{pmatrix} \quad . \tag{5.38}$$

To understand how the time-reversal operator acts on the various terms we note that "physical" operators can be separated into two classes, operators commutating with T_t, like e.g. the position operator:

$$T_t\mathbf{r} = \mathbf{r}T_t \quad , \tag{5.39}$$

and operators anticommutating with T_t, like e.g. the momentum and spin operators:

$$T_t\mathbf{p} = T_t\frac{\hbar}{i}\boldsymbol{\nabla} = -\frac{\hbar}{i}\boldsymbol{\nabla}T_t \quad , \tag{5.40}$$

$$T_t \boldsymbol{\sigma} = -\boldsymbol{\sigma} T_t \quad . \tag{5.41}$$

For the Hamilton operator without an external magnetic field we then have

$$[h, T_t] = 0 \quad , \tag{5.42}$$

which means

$$h\varphi = \epsilon\varphi \quad , \tag{5.43}$$

and

$$h(T_t\varphi) = \epsilon(T_t\varphi) \quad . \tag{5.44}$$

As long as φ and $T_t\varphi$ are linearly independent, both functions are degenerate. According to the definitions given above T_t can be defined by the following equation:

$$T_t = -i\sigma_y K \quad , \tag{5.45}$$

where K is the conjugator

$$K\varphi = \varphi^* \quad . \tag{5.46}$$

One can easily prove that the operator T_t defined this way has the required properties (note: σ_y acts on the two components of a spinor, not on $\mathbf{r}$ or $\boldsymbol{\nabla}$):

$$\begin{aligned} (-i\sigma_y K)\mathbf{r} &= \mathbf{r}(-i\sigma_y K) & (5.47)\\ (-i\sigma_y K)\frac{\hbar}{i}\boldsymbol{\nabla} &= -\frac{\hbar}{i}\boldsymbol{\nabla}(-i\sigma_y K) & (5.48)\\ (-i\sigma_y K)\sigma_x &= -\sigma_x(-i\sigma_y K) & (5.49)\\ &\text{etc.} \end{aligned}$$

In our single-particle problem the spin state is well defined. If we investigate a wave function with "spin up" (in the limit of **j-j**-coupling of the many-body system), we obtain:

$$T_t \begin{bmatrix} \psi \\ 0 \end{bmatrix} = -i\sigma_y K \begin{bmatrix} \psi \\ 0 \end{bmatrix} = \begin{bmatrix} 0 \\ \psi^* \end{bmatrix} \tag{5.50}$$

and analogous for "spin down"

$$T_t \begin{bmatrix} 0 \\ \psi \end{bmatrix} = - \begin{bmatrix} \psi^* \\ 0 \end{bmatrix} \quad . \tag{5.51}$$

Thus we have:

$$T_t^2 \psi(\mathbf{r}, \sigma) = -\psi(\mathbf{r}, \sigma) \quad . \tag{5.52}$$

It is clear that ψ and $T_t\psi$ are orthogonal to each other, wave functions for "spin up" and "spin down", respectively. Therefore, as noted in Eq. (5.43) and (5.44), generally we have that $\varphi_{n,\mathbf{k}}$ and $T_t\varphi_{n,\mathbf{k}}$ are linearly independent functions and that the energy level $\epsilon_n(\mathbf{k})$ is twofold degenerate.

Therefore, the eigenvalue ϵ of a single-particle problem is – independent of spatial symmetry – two-fold degenerate because of time-reversal symmetry:

$$\epsilon_n(\mathbf{k}, \uparrow) = \epsilon_n(-\mathbf{k}, \downarrow) \quad . \tag{5.53}$$

As long as spin polarization can be neglected, we have further:

$$\epsilon_n(\mathbf{k},\uparrow) = \epsilon_n(\mathbf{k},\downarrow) = \epsilon_n(-\mathbf{k},\uparrow) = \epsilon_n(-\mathbf{k},\downarrow) \quad , \tag{5.54}$$

i.e., 4-fold degeneracy!

5.2.3 The Fermi Surface

For metals at $T = 0$K all single particle states with $\epsilon_n(\mathbf{k}) \leq \epsilon_\mathrm{F}$ are occupied. This is in fact the definition of ϵ_F: For a finite N electron system we have $\epsilon_\mathrm{F} = \epsilon_N$. For metals (infinite and periodic) there is a *Fermi surface*. It is defined by the equation

$$\epsilon_n(\mathbf{k}) = \epsilon_\mathrm{F} \quad . \tag{5.55}$$

The Fermi surface is a surface of constant energy in $\mathbf{k}$-space. It separates the occupied from the unoccupied states. The Fermi surface consequently exists only for metals, because, if ϵ_F is in a band gap, condition (5.55) is never fulfilled. Then there is no Fermi surface. At first we investigate the Fermi surface for the example of electrons in jellium. The band

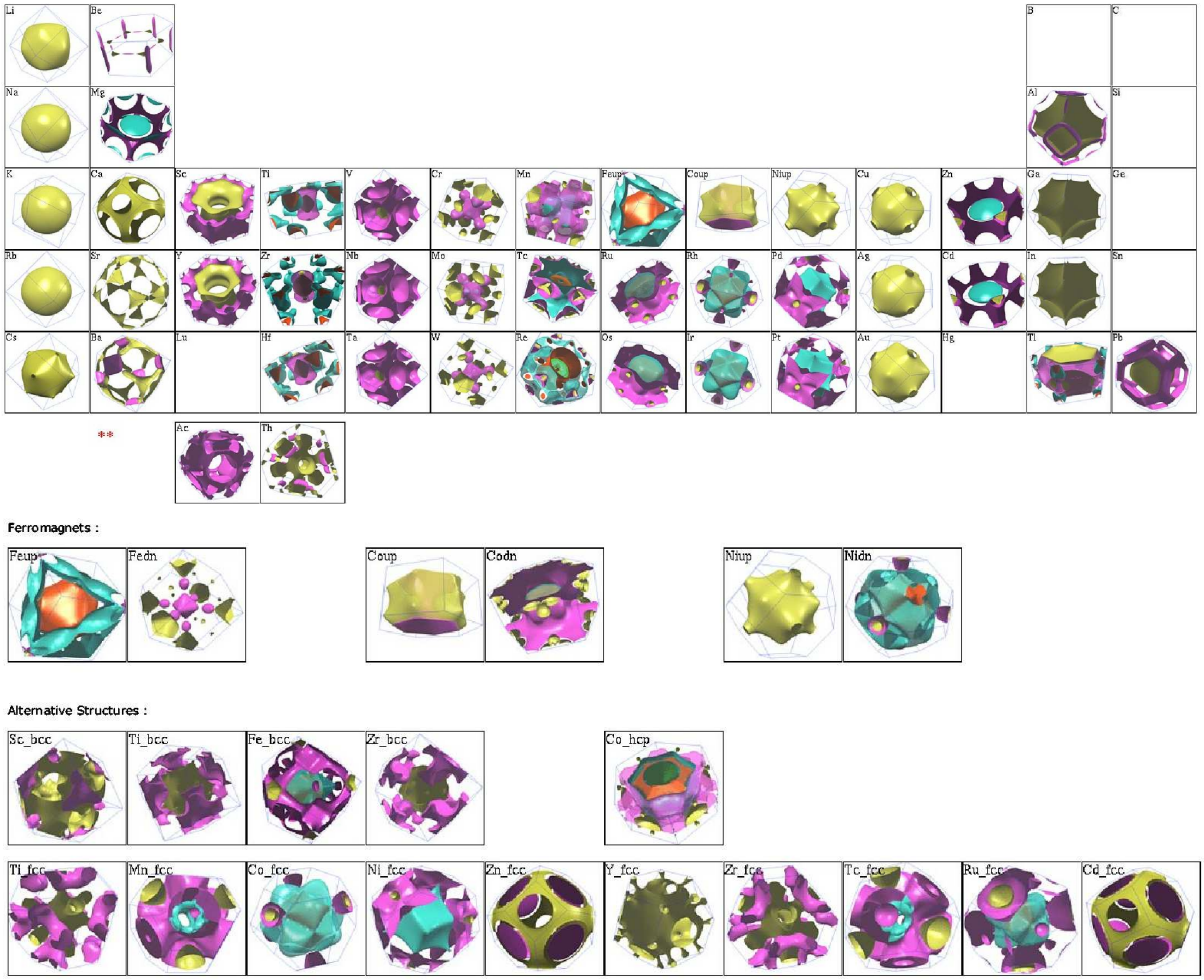

Figure 5.9: The Fermi Surface Database http://www.phys.ufl.edu/fermisurface

structure is given by

$$\epsilon(\mathbf{k}) = \frac{\hbar^2}{2m}k^2 \quad , \tag{5.56}$$

the Fermi-surface is thus the surface of a sphere of radius $|\mathbf{k}| = k_\mathrm{F} = \sqrt{\frac{2m}{\hbar^2}\epsilon_\mathrm{F}}$.

For nearly-free electrons in a periodic system the band structure looks more complicated and the Fermi surface as well. We have:

$$\epsilon_n(\mathbf{k}) = \frac{\hbar^2}{2m}(\mathbf{k}+\mathbf{G}_n)^2 \stackrel{!}{=} \epsilon_\mathrm{F} \quad . \tag{5.57}$$

Sometimes only one band index n will contribute to the Fermi surface, but in general different n will contribute different sections.

And for the realistic materials, i.e., $v^\mathrm{eff}(\mathbf{r}) \neq$ const., the Fermi surface looks again more complicated. Figure 5.9 shows some examples from "The Fermi Surface Database". More details can be found on that webpage.

For the further, very detailed discussion of Fermi surfaces I refer to the Ashcroft-Mermin chapters 9, 14 and 15. This can be presented hardly better than there.

5.3 The LCAO (linear combination of atomic orbitals) Method

In part 5.1 we assumed that the potential of the solid, v^eff, is not particularly strong, and that the band structure is only a weak modification of the dispersion relation of free electrons. This led to the band structure in the approximation of nearly free electrons. This treatment is in principle exact, but typically $v^\mathrm{eff}(\mathbf{r}) = \sum_\mathbf{G} v^\mathrm{eff}(\mathbf{G})e^{i\mathbf{G}\mathbf{r}}$ will have a very large number of Fourier components.

To get a feeling for the wave functions and energies, and for the forces that hold the solid together, also another point of view is possible. For this we now want to start with well separated atoms and investigate what happens if these atoms are brought closer together. In fact the situation present in a solid is rather in the middle between the properties of atoms or molecules and the ones describing the behavior of nearly free electrons. The various modern numerical methods for the calculation of the electronic structure of solids therefore combine both aspects in their methodology. Such methods, in particular the ab initio pseudopotential theory, the linearized muffin-tin orbital method (LMTO) and the linearized augmented plane waves method (LAPW) are discussed in this Chapter.

We start by reminding the reader about the **H_2 molecule**: Since the Hamilton operator (and the potential) has a reflection symmetry, we have: the eigenstates have to be either symmetric or antisymmetric with respect to this reflection plane. If we assume that the molecular eigenstates are linear combinations of the atomic $1s$ states $\hat{\varphi}_{1s}$ (cf. Fig. 5.10),

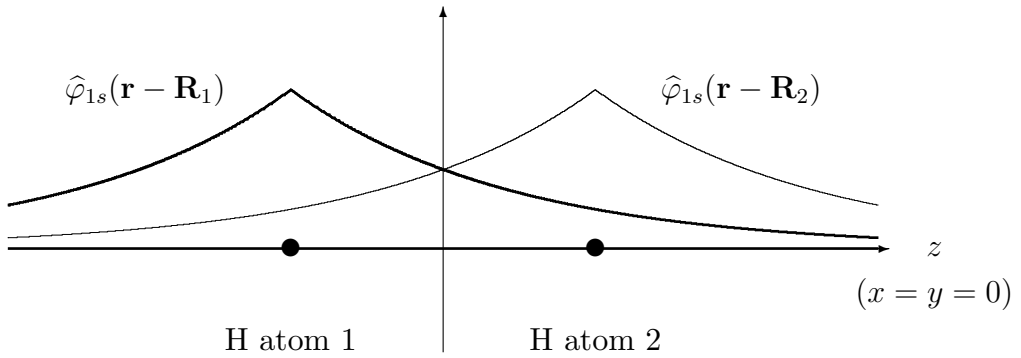

Figure 5.10: Schematic presentation of the atomic eigenstates of two H atoms in the H_2 molecule.

we have

$$\varphi^{\mathrm{b}}_{1s}(\mathbf{r}) = \frac{1}{\sqrt{A}}\left(\hat{\varphi}_{1s}(\mathbf{r}-\mathbf{R}_1)+\hat{\varphi}_{1s}(\mathbf{r}-\mathbf{R}_2)\right) \quad , \tag{5.58}$$

$$\varphi^{\mathrm{a}}_{1s}(\mathbf{r}) = \frac{1}{\sqrt{A}}\left(\hat{\varphi}_{1s}(\mathbf{r}-\mathbf{R}_1)-\hat{\varphi}_{1s}(\mathbf{r}-\mathbf{R}_2)\right) \quad , \tag{5.59}$$

where $1/\sqrt{A}$ ensures the normalization of the φ^{b}, φ^{a} to 1. This is illustrated in Fig. 5.11 and Fig. 5.12 shows the corresponding energy levels.

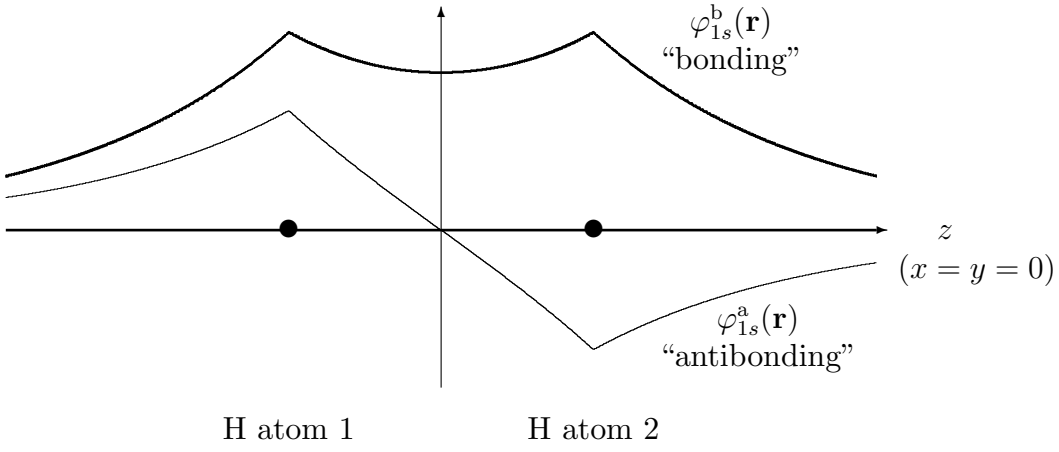

Figure 5.11: Schematic presentation of the electronic eigenstates in the H_2 molecule.

Thus, when the atoms get closer to each other, so that the wave functions start to overlap, there is a splitting of the energy levels:

ϵ_{b} : low energy (thus favored)
φ^{b} : $\oplus\oplus$: the electron density $|\phi_b|^2$ charge has a maximum between the nuclei

ϵ_{a} : high energy (thus unfavored)
φ^{a} : $\oplus\ominus$: the electron density $|\phi_a|^2$ is zero between the nuclei

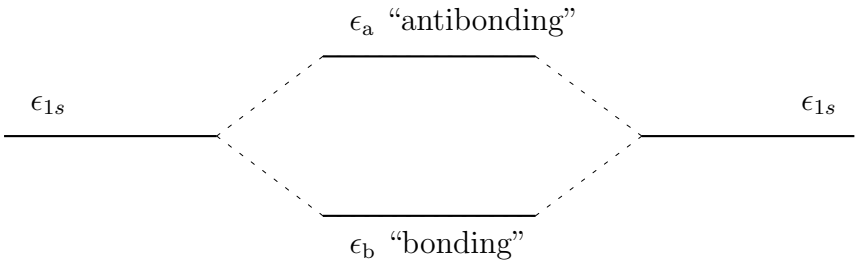

Figure 5.12: Schematic presentation of the electronic energy levels in the H_2 molecule

We now use the same concept to describe a solid, i.e. we use such atom-centered basis functions as basis set. The LCAO basis set for the representation of the wave functions in a solid or molecule is defined by:

$$\chi_\alpha(\mathbf{k},\mathbf{r}) = \frac{1}{\sqrt{A}} \sum_{\mathbf{R}_I}^{M} \boldsymbol{\gamma}_I(\mathbf{k}) \hat{\varphi}_\alpha(\mathbf{r}-\mathbf{R}_I) \tag{5.60}$$

with

M	:	Number of atoms in the base region
$\hat{\varphi}_\alpha(\mathbf{r}-\mathbf{R}_I)$	:	atom-like function, centered at position $\mathbf{R}_I$, (e.g. numerical solution of the atomic Kohn-Sham equation, or Gaussians, or LMTOs with $\alpha = 1s,\ 2s,\ 2p,\ \ldots$)

From the translation invariance in a periodic crystal it follows (Bloch's theorem) that

$$\boldsymbol{\gamma}_I(\mathbf{k}) = e^{i\mathbf{k}\mathbf{R}_I} \quad . \tag{5.61}$$

Thus, there is an infinite number of phases: $e^{i\mathbf{k}\mathbf{R}_I} = +1 \ldots -1$. Here, the value $+1$ refers to $\mathbf{k} = \mathbf{0}$ and the value -1 to the edge of the Brillouin zone: $\mathbf{k} = \frac{1}{2}\mathbf{G}$.

For normalization we choose the condition

$$\langle \hat{\varphi}_\alpha(\mathbf{r}) | \hat{\varphi}_\beta(\mathbf{r}) \rangle = \delta_{\alpha,\beta} \tag{5.62}$$

and

$$A \;=\; M \;=\; \text{number of atoms} \quad . \tag{5.63}$$

This yields that

$$\langle \chi_\alpha(\mathbf{k},\mathbf{r}) | \chi_\beta(\mathbf{k},\mathbf{r}) \rangle \longrightarrow \delta_{\alpha,\beta} \quad ,$$

when the lattice constant goes to ∞.

The eigenfunctions of the single-particle hamiltonian are then written

$$\varphi_n(\mathbf{k},\mathbf{r}) = \sum_\beta c_{n\beta}(\mathbf{k}) \chi_\beta(\mathbf{k},\mathbf{r}) \tag{5.64}$$

and the matrix equation of the Kohn-Sham equation is

$$\sum_\beta \left[h_{\alpha\beta} - S_{\alpha\beta}\epsilon_n(\mathbf{k}) \right] c_{n\beta}(\mathbf{k}) = 0 \quad , \tag{5.65}$$

with

$$
\begin{aligned}
h_{\alpha\beta} &= \langle \chi_\alpha(\mathbf{k},\mathbf{r}) | h | \chi_\beta(\mathbf{k},\mathbf{r}) \rangle && (5.66)\\
&= \frac{1}{M} \sum_{\mathbf{R}_I,\mathbf{R}_J} e^{i\mathbf{k}(\mathbf{R}_I-\mathbf{R}_J)} \langle \hat{\varphi}_\alpha(\mathbf{r}-\mathbf{R}_I) | h | \hat{\varphi}_\beta(\mathbf{r}-\mathbf{R}_J) \rangle \\
&= \sum_{\mathbf{R}_I}^{M} e^{i\mathbf{k}\mathbf{R}_I} \underbrace{\langle \hat{\varphi}_\alpha(\mathbf{r}-\mathbf{R}_I) | h | \hat{\varphi}_\beta(\mathbf{r}) \rangle}_{\epsilon_{\alpha\beta}(\mathbf{R}_I)} && (5.67)
\end{aligned}
$$

$$
\begin{aligned}
S_{\alpha\beta} &= \langle \chi_\alpha(\mathbf{k},\mathbf{r}) | \chi_\beta(\mathbf{k},\mathbf{r}) \rangle && (5.68)\\
&= \sum_{\mathbf{R}_I}^{M} e^{i\mathbf{k}\mathbf{R}_I} \underbrace{\langle \hat{\varphi}_\alpha(\mathbf{r}-\mathbf{R}_I) | \hat{\varphi}_\beta(\mathbf{r}) \rangle}_{s_{\alpha\beta}(\mathbf{R}_I)} \quad . && (5.69)
\end{aligned}
$$

The advantage of the LCAO method, i.e., of using atomic or atom-like orbitals for $\varphi_\alpha(\mathbf{r})$ is that these are very localized. The quantities $\epsilon_{\alpha\beta}(\mathbf{R}_I)$ and $s_{\alpha\beta}(\mathbf{R}_I)$ thus differ from zero only for very few $\mathbf{R}_I$ (often only for $|\mathbf{R_I}| \leq 2$ or 3 interatomic distances). This results in a high numerical efficiency and good scaling with system size. Another advantage of the LCAO method is that the number of basis functions and consequently the dimension of the matrices in Eq. (5.65) can be kept very small. For a solid of hydrogen atoms or of alkali atoms (Na, Cs) as a first approximation (or for a qualitative discussion) it is sufficient to use only one basis function per atom:

$$
\begin{aligned}
\text{H} &: 1s \\
\text{Li} &: 2s \\
&\vdots \\
\text{Cs} &: 6s
\end{aligned}
\qquad (5.70)
$$

For C, Si, Ge, GaAs one has to use at least four orbitals per atom:

$$
\begin{aligned}
\text{C} &: 2s,\ 2p_x,\ 2p_y,\ 2p_z \\
\text{Si} &: 3s,\ 3p_x,\ 3p_y,\ 3p_z \\
&\vdots
\end{aligned}
\qquad (5.71)
$$

The "minimum basis sets" in the examples (5.70) and (5.71) allow for a qualitative description, for a more accurate quantitative description further orbitals have to be included.

What happens, when the atoms get closer to each other? Then the electronic energy levels of the atoms split. This is sketched in Fig. 5.13. For smaller distances the sharp energy levels become *energy bands*. The total number of all states is constant, i.e., independent of the distance of the atoms.

In the spirit of such LCAO basis sets and considering a "minimum basis" we now like to construct the band structure of a simple material.

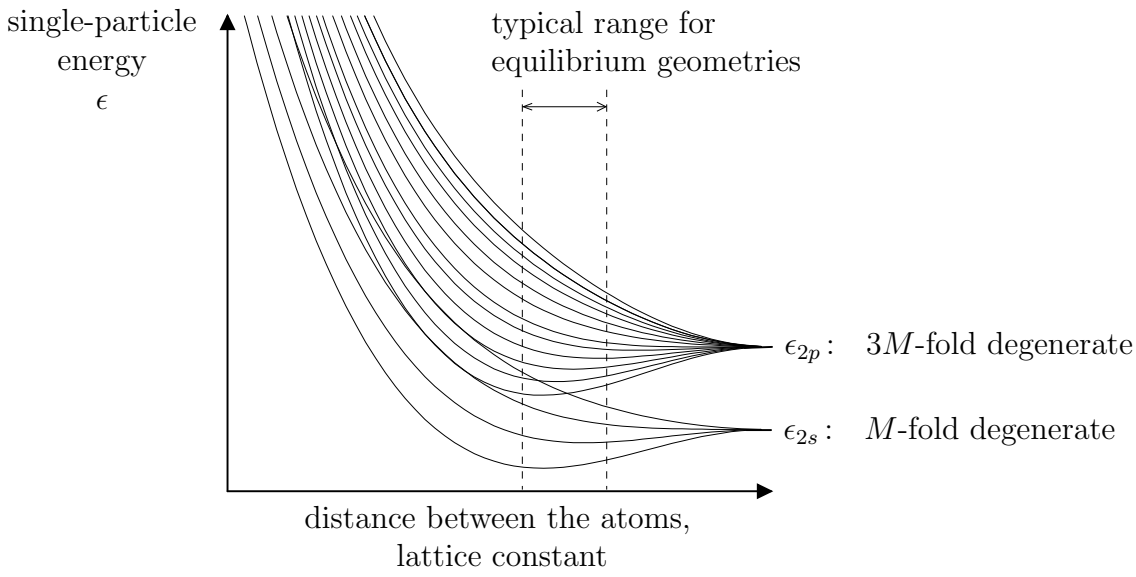

Figure 5.13: Schematic presentation of the energy levels of a solid as function of the interatomic distance. For large distances one obtains the energy levels of the free atoms.

5.3.1 Band Structure and Analysis of the Contributions to Chemical Bonding

We discuss a two-dimensional example. Although in part 5.1 we have used the hexagonal lattice, I now want to talk about the square lattice. Because of the orthogonality of the lattice vectors the discussion is somewhat simpler, cf. Fig. 5.14.

In a qualitative or semi-quantitative description of an s-band we will now just use one s-orbital per atom. An estimate of the relative energies at high symmetry points in the Brillouin zone is compiled in Table 5.1. Knowing about the continuity of the functions $\epsilon_n(\mathbf{k})$ we can now draw the qualitative band structure (Fig. 5.15).

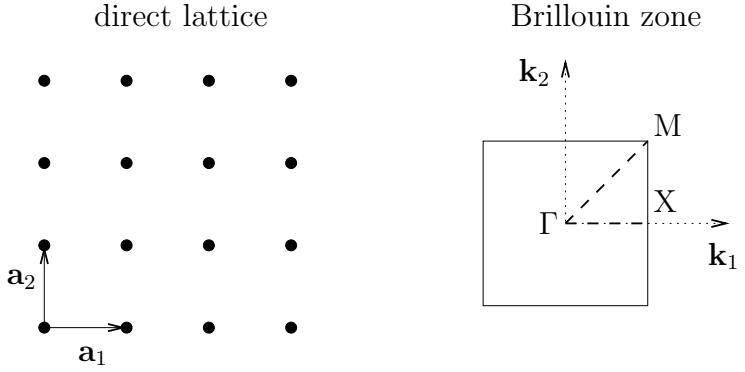

Figure 5.14: The two-dimensional square atomic lattice.

k-point	$\varphi_s(\mathbf{k},\mathbf{r})$	conclusion about the energy
Γ $\mathbf{k}=(0,0)$	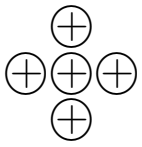	fully bonding $\Rightarrow$ minimum of the energy
X $\mathbf{k}=(\frac{\pi}{a},0)$	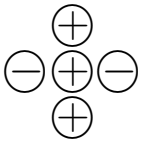	half/ half $\Rightarrow$ mid value energy
M $\mathbf{k}=(\frac{\pi}{a},\frac{\pi}{a})$	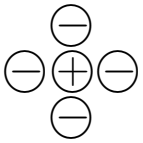	fully antibonding $\Rightarrow$ maximum of the energy

Table 5.1: Schematic picture of the Bloch states of an s-band of a square lattice. Compare with Eq. (5.60) for the basis function, with $\hat{\varphi}_\alpha = s$-orbital. The Bloch state $\varphi_s(\mathbf{k},\mathbf{r})$ is shown at one atom and its four nearest neighbors.

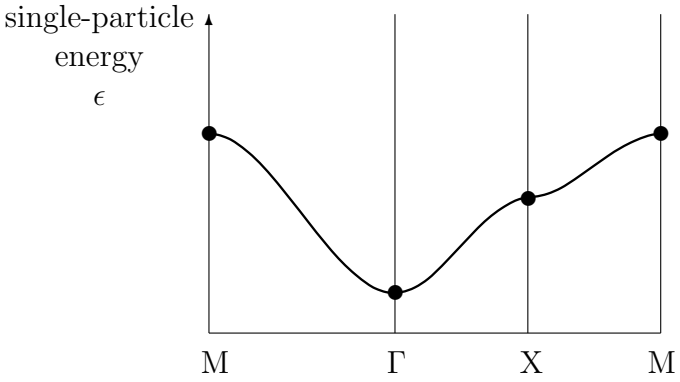

Figure 5.15: Band structure of s-orbitals of the square lattice (qualitative presentation). The dots mark the estimates obtained from Table 5.1.

For the band structure of p-states we discuss p_z (oriented perpendicular to the plane of the lattice) and p_x or p_y separately, because the two types of functions are for a two-dimensional system independent for symmetry reasons: p_z is antisymmetric with respect to the plane of the lattice, p_x and p_y are symmetric with respect to the plane of the lattice.

The illustrations of the wave functions of p_z look qualitatively the same as for s-states (at least when looking from the top on the lattice plane). The dispersion of p_z-orbitals is thus qualitatively the same as that of s-orbitals (cf. Fig. 5.15).

In Fig. 5.16 we summarize the results for these p_x, p_y-states, of the p_z-, and of the lower-lying s-states to the band structure shown in Fig. 5.16. We recognize that this band structure is similar to the result of nearly free electrons. The s- or p-band is similar to a

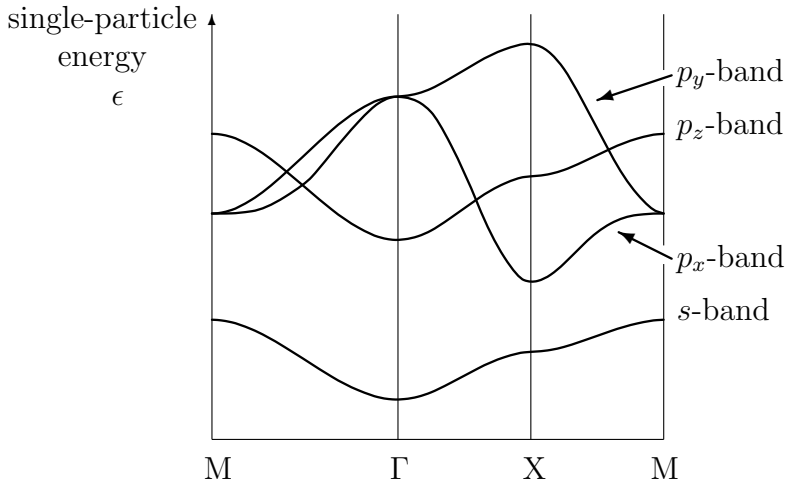

Figure 5.16: Band structure of s- and p- states in the square lattice (qualitative representation, the relative position of the p_z band with respect to the p_x-, p_y-band is chosen arbitrarily).

k-point	$\varphi_{p_x}(\mathbf{k},\mathbf{r})$	$\varphi_{p_y}(\mathbf{k},\mathbf{r})$
Γ $\mathbf{k}=(0,0)$	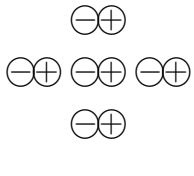	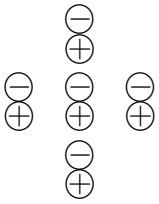
	strongly antibonding	strongly antibonding
X $\mathbf{k}=(\frac{\pi}{a},0)$	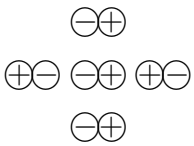	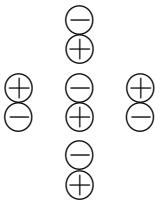
	fully bonding	fully antibonding
M $\mathbf{k}=(\frac{\pi}{a},\frac{\pi}{a})$	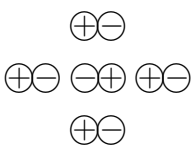	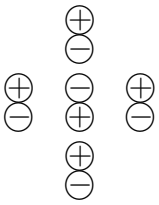
	strongly bonding	strongly bonding

Table 5.2: Schematic picture of the Bloch states of the p_x- and p_y-bands of a square lattice. Compare with Eq. (5.60) for the basis functions, with $\hat{\varphi}_\alpha = p_x$- or p_y-orbital. The Bloch states $\varphi_{p_x}(\mathbf{k},\mathbf{r})$ and $\varphi_{p_y}(\mathbf{k},\mathbf{r})$ are shown at one atom and its four nearest neighbors.

parabola of free electrons, reduced to the 1st Brillouin zone and split at the points satisfying the Bragg-condition. This can also be shown mathematically, because a plane wave can be expanded in spherical harmonics:

$$e^{i\mathbf{kr}} = 4\pi \sum_{l=0}^{\infty} \sum_{m=-1}^{l} i^l \sqrt{\frac{\pi}{2kr}} J_{l+1/2}(kr) Y_{lm}^*(\Omega_{\mathbf{k}}) Y_{lm}(\Omega_{\mathbf{r}}) \quad , \tag{5.72}$$

with $\Omega_{\mathbf{k}}$ and $\Omega_{\mathbf{r}}$ labelling the spatial angle and $J_{l+1/2}$ representing the Bessel function of index $l + \frac{1}{2}$.

The above discussion and explanation of the band structure clarifies the meaning of the quantum number $\mathbf{k}$. It describes the phase difference of orbitals that are centered at different atoms, and $\lambda = \frac{2\pi}{|\mathbf{k}|}$ is the wave length of the wave function. In a diatomic molecule there are only two phases: bonding and antibonding (or $+1$ and -1). In a crystalline solid there are an infinite number of phases covering the full range from "bonding" to "antibonding" with respect to the nearest neighbor interaction. The more bonding states are occupied (compared to antibonding states) the stronger bound (the more stable) is the material (e.g. Fe has a higher cohesive energy than Cu).

5.4 The Density of States, $N(\epsilon)$

The density of states is defined as the number of states per unit volume at the energy ϵ:

$$N(\epsilon) = \sum_n \frac{2}{(2\pi)^3} \int\limits_{1.\mathrm{BZ}} \delta(\epsilon - \epsilon_n(\mathbf{k})) d^3k \quad . \tag{5.73}$$

We want to write $N(\epsilon)$ differently to point out the characteristic structure, which enables a relatively direct comparison between band structure and density of states.

For this purpose we write the number of states per unit volume $[\epsilon, \epsilon + d\epsilon]$ as follows:

$$N(\epsilon)d\epsilon = \sum_n N_n(\epsilon)d\epsilon \quad , \tag{5.74}$$

where n is the band index and $N_n(\epsilon)$ the density of states of the band n. Then we have:

$$N_n(\epsilon)d\epsilon = \frac{2}{(2\pi)^3} \int\limits_{1.\mathrm{BZ}} d^3k \cdot \begin{cases} 1 & \text{if} \quad \epsilon \le \epsilon_n(\mathbf{k}) \le \epsilon + d\epsilon \\ 0 & \text{otherwise} \end{cases} \quad . \tag{5.75}$$

This is a volume integral in $\mathbf{k}$-space, which is enclosed by the surfaces $\epsilon_n(\mathbf{k}) = \epsilon$ and $\epsilon_n(\mathbf{k}) = \epsilon + d\epsilon$. $\delta\tilde{k}(\mathbf{k})$ shall be the distance of these two surfaces perpendicular to the first surfaces. Then we have:

$$N_n(\epsilon)d\epsilon = \frac{2}{(2\pi)^3} \int\limits_{\epsilon_n(\mathbf{k})-\epsilon=0} \delta\tilde{k}(\mathbf{k}) df \quad , \tag{5.76}$$

and we obtain

$$N_n(\epsilon)d\epsilon = \frac{2}{(2\pi)^3} \int\limits_{\epsilon_n(\mathbf{k})-\epsilon=0} \frac{1}{|\boldsymbol{\nabla}_{\mathbf{k}} \epsilon_n(\mathbf{k})|} df \quad , \tag{5.77}$$

because

$$\boldsymbol{\nabla}_{\mathbf{k}}\epsilon_n(\mathbf{k}) = \frac{\partial\epsilon_n(\mathbf{k})}{\partial\tilde{k}(\mathbf{k})} \cdot \hat{\mathbf{n}}(\mathbf{k}) \quad , \tag{5.78}$$

where $\hat{\mathbf{n}}$ is the unit vector with a direction perpendicular to $\epsilon_n(\mathbf{k}) = \epsilon$.

Characteristic structures occur at energies where the gradient in the denominator of Eq. (5.77) becomes zero. These positions are also called *Van-Hove singularities*. Examples for such singularities are given in Fig. 5.17. For three-dimensional systems these divergences in the integrand can be integrated.

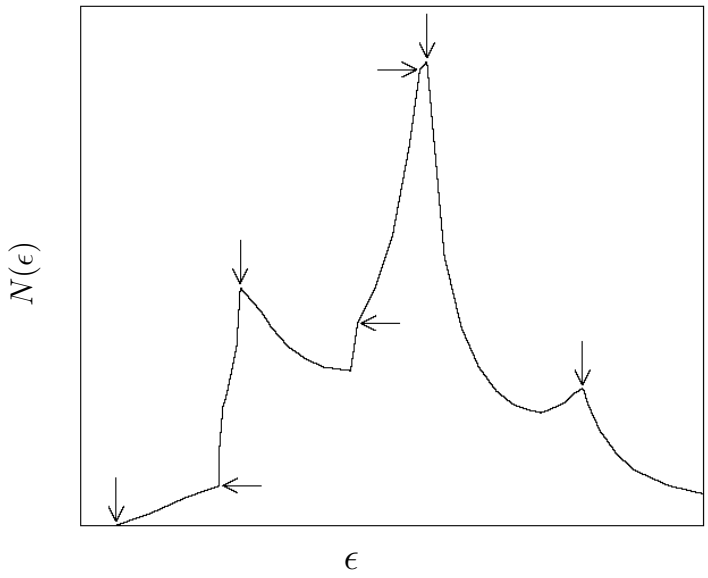

Figure 5.17: The density of states of a band. Singularities in the density of states can be identified (arrows).

5.5 Other Methods for Solving the Kohn-Sham Equations of Periodic Crystals

To be completed later.For now see:
http://wwwitp.physik.tu-berlin.de/ekreide/ss08/TFP/2008-05-27/pdf/lect_col.pdf

5.5.1 The Pseudopotential Method

To be completed later. For now see:
http://wwwitp.physik.tu-berlin.de/ekreide/ss08/TFP/2008-05-27/pdf/lect_col.pdf

5.5.2 APW and LAPW

To be completed later. For now see:
http://wwwitp.physik.tu-berlin.de/ekreide/ss08/TFP/2008-05-27/pdf/lect_col.pdf

5.5.3 KKR, LMTO, and ASW

To be completed later. For now see:
http://wwwitp.physik.tu-berlin.de/ekreide/ss08/TFP/2008-05-27/pdf/lect_col.pdf

5.6 Many-Body Perturbation Theory (beyond DFT)

To be completed later. For now see:
http://wwwitp.physik.tu-berlin.de/ekreide/ss08/TFP/2008-05-27/pdf/lect_col.pdf